

The isotope effect in solvation dynamics and nonadiabatic relaxation: A quantum simulation study of the photoexcited solvated electron in D₂O

Benjamin J. Schwartz^{a),b)} and Peter J. Rossky

Department of Chemistry and Biochemistry, University of Texas at Austin, Austin, Texas 78712-1167

(Received 16 April 1996; accepted 12 July 1996)

Quantum nonadiabatic molecular dynamics simulations are used to explore the molecular details surrounding photoexcitation of solvated electrons in deuterated water. The results are compared to previous studies in normal water [B. J. Schwartz and P. J. Rossky, *J. Chem. Phys.* **101**, 6902, 6917 (1994)] to elucidate the nature of the isotope effect on both the solvation and nonadiabatic relaxation dynamics. The solvent spectral density couples differently to the individual energy levels than to the quantum energy gap, indicating the importance of the symmetry of both the ground and excited states in determining the resulting solvent response. The solvation dynamics are characterized by a Gaussian plus biexponential decay. Deuteration has little effect on the Gaussian component or long time exponential decay of the solvent response function, but a ~20% isotope effect is observed on the faster exponential decay. The solvent response following nonadiabatic relaxation is found to be much more rapid than that following photoexcitation, reflecting the importance of short range mechanical forces and molecular shape in solvation dynamics. Simulated spectral dynamics of the individual ground state bleach, excited state absorption, and stimulated emission components in deuterated water are presented and the results compared to those in normal water. The spectral isotope dependence results principally from the difference in calculated nonadiabatic relaxation rates, which are a factor of ~2 slower in D₂O than H₂O. Using the fact that a separate analysis of the quantum decoherence times for the electron suggests that the nonadiabatic transition rates in the two solvents should be identical, calculated spectral transients are corrected for the case of identical nonadiabatic lifetimes and show essentially identical behavior in light and heavy water, in agreement with current experimental results. The small isotope effect on the solvation response should be observable with higher time resolution. © 1996 American Institute of Physics. [S0021-9606(96)51339-5]

I. INTRODUCTION

The dynamics of a chemical reaction in solution are critically affected by solvent molecules whose motions are coupled to the reactant energy levels. This solute-solvent coupling can alter chemistry in two principle ways. The first way is through solvation dynamics, the response of the solvent to changes in the electronic charge distribution of the reacting species.¹⁻³ Since all chemical reactions involve the rearrangement of electrons, the time scale over which the solvent acts to stabilize new charge distributions can determine whether or not (or how rapidly) a particular reaction can cross its transition state. The second way is through nonadiabatic coupling, the mixing of the adiabatic potential surfaces of the reacting species due to rapid nuclear motions of the solvent.⁴ By allowing for transitions between quantum energy levels, nonadiabatic coupling provides a reacting system access to entirely new regions of phase space, permitting the creation of new products or altered reaction rates. These two types of solvent effects on chemical reactivity are not entirely independent: as the charge distribution changes during a reaction, solvation dynamics will determine the evolu-

tion of the new adiabatic energy levels and the extent to which they are coupled nonadiabatically. In this paper, we will utilize the isotope effect to explore the connections between solvation dynamics and nonadiabatic relaxation for a model condensed phase quantum system, the hydrated electron.

The hydrated electron serves as an excellent paradigm for the study of aqueous solvent effects on chemical reactivity.⁵⁻³⁰ Because the excess electron resides in a roughly spherical solvent cavity, its eigenstates are similar to those of a particle in a spherical box.⁵⁻⁷ The coupling between the solvent and the solute for this system is manifest in three ways. First, solvent molecular motions distort the size and shape of the cavity, directly modulating the electronic energy levels. Second, upon promotion to the first excited state, solvent motions act to accommodate the new *p*-like charge distribution, dynamically decreasing the quantum energy gap. Finally, as solvation brings the ground and excited states closer together in energy, nonadiabatic coupling due to rapid solvent motions causes a radiationless transition back to the ground state. These three aspects of the extremely strong solute-solvent coupling in this system are reflected spectroscopically in the breadth of the equilibrium absorption band, in the enormous fluorescence Stokes shift following photoexcitation, and in the rapid recovery of the equilibrium absorption spectrum following radiationless relaxation,

^{a)}Present address: Inst. for Polymers and Organic Solids, University of California, Santa Barbara, CA 93106-5090.

^{b)}Permanent address: Dept. of Chemistry and Biochemistry, University of California, Los Angeles, CA 90095-1569.

respectively.^{5–10} This spectroscopic accessibility and the theoretical simplicity of the hydrated electron have made it the first system where condensed phase nonadiabatic simulation and experiment have successfully converged.²

Recent femtosecond laser experiments by Barbara and co-workers have measured the dynamical spectral changes following photoexcitation for the hydrated electron system.^{27–30} In these three laser pulse experiments, hydrated electrons are produced by an initial synthesis pulse through multiphoton ionization of neat water or photodetachment of a negative ion. After several nanoseconds delay to ensure equilibration in the ground state, the electrons are promoted to their first excited state with a second femtosecond laser pulse. The spectral changes due to solvation and nonadiabatic relaxation following this photoexcitation are recorded with a third ultrashort pulse at a variety of wavelengths. Because of the temporal width of the pulses and optical dispersion in the sample, the time resolution of these experiments is limited to ~ 300 fs. The experiments measured solvation and nonadiabatic relaxation time scales of ≤ 300 fs and ~ 1.1 ps, and found no direct evidence for simple two-state (isobestic) kinetic behavior. In addition, when similar experiments were performed in deuterated water, no isotope effect was observed on any of the dynamics within the time resolution of the apparatus.^{28,29}

In previous work,^{7–10} we simulated the experiments of Barbara and co-workers by treating the hydrated electron at a fully quantum mechanical level. Following photoexcitation, we found that the electron occupies a *p*-like state with lobes oriented along the long axis of the solvent cavity. The solvent responds on ~ 25 fs Gaussian and ~ 250 fs exponential time scales to create a more peanut-shaped cylindrically symmetric cavity. The electron grows by a factor of ~ 2 along the cavity long axis, and solvent molecules are brought into the nodal region near the electron center of mass. These solvent motions leave the energy of the occupied excited state roughly unchanged, but increase the energies of the ground state and the higher lying excited states. By analyzing the transient spectroscopy in terms of ground state bleach, excited state absorption, and stimulated emission components, we were able to assign the observed spectral dynamics in terms of specific solvent motions inducing changes in the frequencies and oscillator strengths of the underlying quantum transitions.⁸ The lack of observed isobestic behavior results from solvation-induced changes in the absorption and bleach spectral components during the course of the radiationless relaxation.⁹ In addition, we found a roughly inverse-linear dependence of the nonadiabatic transition rate on the magnitude of the evolving quantum energy gap.⁷ Based on these results, we assigned the 300 fs and 1.1 ps spectroscopic time scales to excited state solvation dynamics and nonadiabatic relaxation, respectively,^{7–9} rather than to nonadiabatic relaxation followed by ground state solvation as previously suggested.^{27,28}

In this paper, we extend our previous studies on the hydrated electron system to investigate the isotope effect on solvation dynamics and nonadiabatic relaxation. In Sec. II we outline the nonadiabatic quantum methods used for simu-

lating the photoexcited solvated electron in D₂O. Section III explores in detail the nature of the solvent fluctuations coupled to the hydrated electron. The solvent response for the solvated electron in deuterated water is examined and compared to previous experimental, theoretical, and simulation studies of the isotope effect on solvation. The presence of only a small isotope effect on the inertial portion of the solvent response indicates a large degree of translational character to the initial solvent molecular motions. In Sec. IV, we examine the isotope effect on the nonadiabatic relaxation of the hydrated electron. In contrast to experiment, we find internal conversion rates which are a factor of ~ 2 slower in D₂O than in H₂O, a result which stems from incorrect choice of the quantum decoherence time in the nonadiabatic dynamics algorithm. We explore the molecular nature of the solvent dynamics following radiationless relaxation, and find a significant difference between the solvent responses following photoexcitation and nonadiabatic relaxation. This difference is rationalized by considering the role of solvent mechanical forces (dispersion and Pauli repulsion) in competition with the Coulomb forces responsible for dielectric solvation. Section V presents the calculated ultrafast spectroscopic transients for the solvated electron in D₂O. The individual bleach, absorption, and stimulated emission spectral components are analyzed and compared to those investigated previously in H₂O. Using a simple model for the connection between the nonadiabatic transition rate and the solvation dynamics, we correct the calculated spectroscopy in D₂O for the case where the nonadiabatic transition rates in the two solvents are identical. In agreement with experiment, we demonstrate that at 300 fs time resolution, there would be no measurable spectroscopic differences between the ultrafast transients in light and heavy water for comparable transition rates. Finally, Sec. VI summarizes all of these results, and points out directions for future experiments with improved time resolution.

II. METHODS

The nonadiabatic simulation procedures we employ are identical to those used in our previous studies of photoexcitation of the solvated electron in H₂O,^{7–13} and have also been described in detail in the literature.^{31–33} Briefly, the model system consists of one quantum mechanical electron and 200 classical deuterated water molecules in a cubic cell with standard periodic boundary conditions at room temperature. The electron–D₂O interactions were described with a pseudopotential,³⁴ which contains terms accounting for the Coulomb interaction between the solvated electron and the partial charges on the D and O atoms of the solvent molecules, the polarization interaction between the solvent molecules and the solvated electron, and the orthogonality requirement between the wave functions of the solvated electron and the electrons in the solvent molecular orbitals. This potential is identical to that used in our previous work on H₂O, and is discussed in detail elsewhere.³⁴ The equations of motion were integrated using the Verlet algorithm³⁵ with a 1 fs time step in the microcanonical ensemble. The adiabatic

eigenstates at each time step were calculated via an efficient iterative and block Lanczos scheme³¹ utilizing a 16^3 plane wave basis; the lowest 6 eigenstates were computed during nonadiabatic dynamics, and the lowest 40 eigenstates were employed in all spectral computations. All spectra presented here were smoothed in the frequency domain with a 1:2:1 filter, and then convoluted with a 300 fs Gaussian to provide for better comparison to experiment as well as to ensure the correct statistical weights in the ensemble average.⁸

The starting point of the simulations was an equilibrated configuration of the electron in H₂O, with the masses, velocities, and box size scaled to produce the model of the electron in D₂O. The deuterated system was then equilibrated for 10 ps with velocity rescaling every 100 fs for the first 5 ps and every 500 fs for the latter 5 ps. After an additional 10 ps equilibration with no velocity rescaling, a 40 ps adiabatic ground state trajectory was run (a portion of which is shown in Fig. 1). This ground state trajectory was divided into twenty 2 ps intervals, and the first configuration in each interval which had a quantum energy gap resonant with the experimental excitation energy³⁶ was used as the launching point for nonadiabatic excited state trajectories. Each trajectory was run through its nonadiabatic transition to the ground state, and the ground state dynamics were subsequently followed for an additional 0.5 ps.³⁷

Nonadiabatic dynamics were performed using the algorithm of Webster *et al.*,^{31,32} which is based on a combination of the stochastic surface hopping scheme of Tully and Preston³⁸ and the nonadiabatic scattering formalism of Pechukas.³⁹ In this approach, nonadiabatic transition probabilities are computed as the squares of the (complex) overlaps of the occupied state at one time step with the adiabatic basis at the following time step. Weighted by these transition probabilities, the final state for the new time step is selected stochastically. The Pechukas expression is then used to self-consistently determine the dynamics of the classical particles associated with the given initial and chosen final quantum states, allowing for smooth evolution during quantum transitions. Because the myriad of classical paths associated with each possible final state can interfere, “memory” of the complex transition amplitudes is lost after a certain time, an effect known as quantum decoherence.^{33,40} In our present application of the Webster *et al.* algorithm, we chose to drop the complex phases of the nonadiabatic transition amplitudes at the end of each time step to account for this decoherence. Thus, the comparisons presented here between nonadiabatic dynamics in H₂O and D₂O are based on identical decoherence times in the two solvents. Our choice was based in part on the recent semiclassical golden rule calculations of Neria and Nitzan,^{15,16} who found little change in the decay of quantum coherence upon isotopic substitution for the hydrated electron system. More recently, however, we reinvestigated the role of quantum coherence in this system and determined that electrons in deuterated water should have a decoherence time which is ~50% longer than that in normal water.³³ The implications of this difference in decoherence times are discussed in detail elsewhere,³³ and we will return to the effect of decoherence on the nonadiabatic transition rate in Sec. IV.

The classical model we use for D₂O is a modification of the flexible version of the simple point charge (SPC) model for water due to Toukan and Raman.⁴¹ We utilize the same inter- and intramolecular parameters as Toukan and Raman, but choose a deuteron mass of 2 amu instead of the proton mass of 1 amu. We also slightly adjusted the box size in our simulation (to 18.19 from 18.17 Å) to match the experimental solvent density of 1.104 g/ml at 300 K. We selected this model to allow for direct comparison to our earlier H₂O work, even though to the best of our knowledge, the properties of this particular model for D₂O have not been explored previously. Several models of isotopically substituted water have been well-characterized,^{42–44} however, including a flexible version of SPC which differs from the model we employ only in that it uses harmonic interactions for the intramolecular degrees of freedom.⁴⁴ Most of these models find that the translational diffusion coefficient of water increases by a factor of ~1.2 upon isotopic substitution, in good agreement with the experimental isotope shift of 1.23 at 300 K.⁴⁵ Perhaps of more relevance for solvation dynamics are the dielectric relaxation and rotational correlation times. The Debye relaxation times for rigid models of deuterated water are only 5%–12% larger than those for normal water,^{42,43} in relatively poor agreement with the experimental finding of a 26% increase. The flexible model for D₂O most similar to ours,⁴⁴ however, shows a ~20% increase in the self-reorientation time about the dipole axis upon deuteration, in much better agreement with experiment.

In comparing our model for D₂O to experiment, it is important to note that no classical simulation model will adequately reproduce quantum effects which are important in a protonated fluid like water. Classically, the static ensemble properties for light and heavy water should be identical since the two fluids contain identical nuclear configurations with identical statistical weights. The only differences in the ensemble properties of classical H₂O and D₂O should be in dynamical quantities such as time correlation functions which depend on the rate at which these fluids sample their configurations. Quantum mechanically, however, the dispersion of the deuteron is much less than that of the proton. As a result, real (quantum mechanical) D₂O has stronger hydrogen bonding and is a more ordered fluid than H₂O at the same temperature.⁴⁶ One manifestation of this extra ordering is a ~15 nm blueshift of the equilibrium absorption spectrum of the hydrated electron upon deuteration.⁴⁷ Our semiclassical models for the electron in the two solvents have identical solvent configurations and interaction potentials; as a result, the calculated ground state absorption spectra in the two classical solvents are identical within statistical limits (cf. the reference spectra for D₂O in Figs. 8 and 9 with our previously calculated H₂O spectrum in Fig. 1 of Ref. 7). In addition to missing this small shift in the spectroscopy, our semiclassical model for the solvated electron would not reproduce any quantum effects that might be important to solvation or to the energy partitioning and coupling in nonadiabatic dynamics. With these caveats in mind, we explore the classical isotope effect on the solvation dynamics of the solvated electron in Sec. III.

III. LINEAR RESPONSE AND THE ISOTOPE EFFECT ON SOLVATION DYNAMICS

The importance of the solvent's response to the changing electronic charge distribution during a chemical reaction has prompted an explosion of recent experimental, theoretical, and simulation studies of solvation dynamics.¹⁻³ The effects of solvent fluctuations on the quantum energy gap of a quantum solute, $U(t) = E_{\text{exc}}(t) - E_{\text{gnd}}(t)$, are described by the equilibrium solvent response function

$$C(t) = \frac{\langle \delta U(0) \delta U(t) \rangle}{\langle (\delta U)^2 \rangle} \quad (1)$$

where $\delta U(t) = U(t) - \langle U \rangle$ is the fluctuation of the gap from its average value and the angled brackets denote an equilibrium ensemble average. In the limit of linear response, the regression of fluctuations resulting from a perturbation should relax in the same manner as those present at equilibrium. Thus, for small perturbations, the nonequilibrium solvent response function

$$S(t) = \frac{\bar{U}(t) - \bar{U}(\infty)}{\bar{U}(0) - \bar{U}(\infty)} \quad (2)$$

should be identical to $C(t)$ in Eq. (1). The overbars in Eq. (2) denote a nonequilibrium ensemble average. In a typical solvation experiment, a probe molecule (usually an organic dye) has its charge distribution changed by photoexcitation, and the time dependent fluorescence Stokes shift is monitored. The nonequilibrium response function $S(t)$ is then determined by approximating the quantum energy gap as the peak or first moment of a log-normal fit to the instantaneous fluorescence spectrum.⁴⁸ The relationship between this spectroscopically determined solvent response and the time evolution of the underlying quantum energy gap has been explored previously for the hydrated electron system.¹¹

The solvent fluctuations which modulate the quantum energy gap of a solute take place at the frequencies present in the solvent's spectral density. There has been a great deal of interest in the solvent spectral density for water in particular, including investigations by infrared absorption,⁴⁹ depolarized Raman scattering,⁵⁰ the optical Kerr effect,^{51,52} and molecular dynamics simulation.^{53,54} The spectral density of liquid water is roughly characterized by high frequency intramolecular symmetric and antisymmetric stretching (3200–4000 cm⁻¹) and bending motions (1500–1800 cm⁻¹), as well as lower frequency intermolecular librational (400–1000 cm⁻¹) and various hindered translational motions (~60 and ~175 cm⁻¹). As expected upon deuteration, the bending, stretching, and librational motions are decreased in frequency by $\sim\sqrt{2}$, while the lower frequency translational motions show relatively little change upon isotopic substitution. All of these different solvent motions can modulate the solute quantum energy levels; thus, the overall isotope effect on solvation dynamics will depend on the interplay between these motions and how strongly each couples to the energy levels of the solute.

Figure 1 shows a 1.5 ps slice of the ground state equilibrium trajectory of the solvated electron in D₂O. The lower

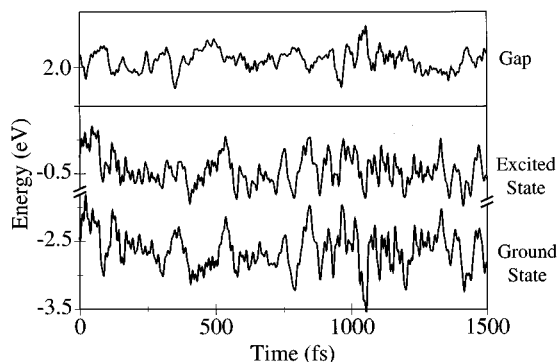


FIG. 1. Dynamical history of the lowest two adiabatic energy levels and the quantum energy gap for a 1.5 ps portion of the ground state trajectory describing the solvated electron in deuterated water. The y axis scale is identical for all three curves; the scale breaks are included for ease of comparison. The upper curve representing the quantum energy gap is the difference of the lower two curves depicting the ground and first excited adiabatic eigenstates.

curve depicts the energy of the electronic ground state, while the center curve shows the energy of the lowest *p*-like excited state to which photoexcitation occurs. The effect of strong coupling to solvent motions is readily evident—the energy levels vary by nearly 0.5 eV on a time scale of a few tens of femtoseconds. Clearly visible are rapid oscillations at the O–D stretching frequencies with a period of ~ 15 fs as well as slower modulations at the bending and intermolecular solvent frequencies. It is interesting to note that the two energy levels often tend to be modulated together; that is, some particular solvent motions which affect the energy of the ground state affect the energy of the excited state in the same fashion. Thus, especially on short time scales, the two curves fluctuate largely in parallel. The upper curve in Fig. 1 shows the time evolution of the quantum energy gap, the difference between the ground and excited state energies, on the same energy scale as the lower two curves (note the scale break in the lower part of Fig. 1; the average gap is around 2 eV). Because some types of solvent fluctuations affect the two individual states in the same manner, the fluctuations in the quantum gap are both quantitatively and qualitatively quite different from those of the individual energy levels.

The fluctuations which appear in the time evolution of the quantum energy gap are due only to those solvent modes which are significantly displaced upon excitation. A simple Fourier analysis shows that the fluctuations present in the individual energy levels are well matched to the bulk solvent spectral density, including contributions from both the intra- and intermolecular degrees of freedom. The quantum energy gap, however, shows essentially no modulation at either the solvent stretch or bend frequencies, and shows a small enhancement of the translational motions relative to the librational motions compared to the neat solvent spectral density.⁵⁵ This can be easily rationalized with a simple physical picture. Upon photoexcitation from the *s*-like ground state, the charge density in the *p*-like excited state “pushes” on solvent molecules along the angular lobes, and stops pushing on those molecules which are now aligned

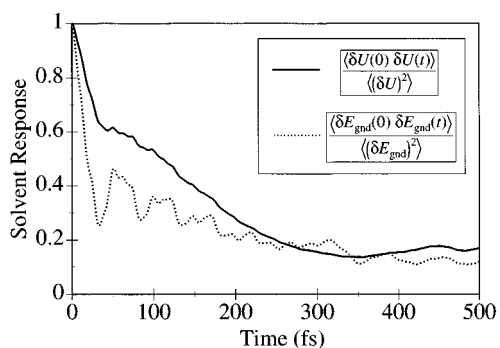


FIG. 2. Linear response predictions [Eq. (1)] for solvation dynamics based on the autocorrelation of the equilibrium quantum energy gap fluctuations (solid curve) and the equilibrium ground state energy fluctuations alone (dashed curve) for the solvated electron in D₂O.

with the nodal region between the lobes. Since the electron is large (~ 4 Å diam) compared to the size of the solvent, this pushing motion acts not just on single atoms but instead acts fairly uniformly over entire water molecules. Thus, the relatively stiff intramolecular O–D stretching and bending motions are not much affected by this change in charge distribution, but the softer hindered translational and rotational motions of the entire molecule are altered.

The difference in fluctuations between the individual energy levels and the quantum energy gap is further explored in Fig. 2. The solid curve shows the autocorrelation of the quantum energy gap, which is also the linear response prediction [Eq. (1)] for the solvation dynamics following excitation, averaged over all 40 ps of the ground state trajectory. The dotted curve shows a similar autocorrelation of the electronic ground state energy alone (the autocorrelation of the energy fluctuations of the individual *p*-like excited states are nearly identical). The two curves are clearly different, reflecting the different composition of solvent modes present in the underlying fluctuations.

The regression of the ground state fluctuations shows a fast initial decay, followed by a pronounced ringing at the D₂O librational frequency. This type of librational oscillation has been previously observed in the solvation dynamics of water by Maroncelli and Fleming.⁵⁶ In their simulations, Maroncelli and Fleming examined aqueous solvation dynamics by changing the overall charge of an atomic probe. Like these charged atomic solutes, the ground state of the hydrated electron is spherically symmetric, and the oscillations in the ground state solvent response indicate the importance of collective water librational motions in coupling to spherically symmetric charge distributions. For the hydrated electron, however, the photoexcitation changes the symmetry of the charge distribution. Because the orientation of water dipoles around the electronic ground state is already nearly favorably aligned for solvation of the lobes of the excited state, collective librational motions are not as effective in relaxing the new excited state charge distribution;⁵⁷ these librational motions which strongly modulate the individual states make a smaller contribution to the autocorrelation of the quantum energy gap. Thus, the symmetry of the charge

distribution involved is important to determining the effectiveness of the various modes in solvation dynamics.

This symmetry dependence to the solvation dynamics has also been observed in previous simulation studies. Kumar and Maroncelli⁵⁸ recently observed differing solvent responses for a benzenelike solute with different excited states having various order multipolar charge distributions.⁵⁹ In our earlier work studying the polarization dependence of the transient spectroscopy of the hydrated electron, we found that solvent fluctuations with different symmetries can cause relaxation on very different time scales.¹⁰ This symmetry dependence to the solvation dynamics has important implications for linear response. We note that like in H₂O,⁷ solvation of the photoexcited solvated electron in D₂O falls in the linear regime: the autocorrelation of the energy gap decays in an almost identical fashion to the nonequilibrium solvent response following photoexcitation (cf. Fig. 3). Figure 2, however, indicates that considerable caution is necessary in using ground state potential fluctuations for linear response predictions of solvation dynamics. Depending on the nature of the excited state involved, fluctuations of the quantum energy gap can behave very differently from fluctuations of either the ground state or excited state energies alone. In other words, the detailed nature of the solute makes the spectrum of couplings between the solvent spectral density and the solute electronic energy gap nonuniform (in this case, damping out the intramolecular modes and heavily weighting the hindered translational motions).

The relationship between solvent–solute interaction symmetry and the nature of solvent motions in solvation dynamics has also been recently explored in a detailed theoretical analysis by Ladanyi and Stratt.⁶⁰ By making a scaling argument in a solvation theory based on instantaneous normal modes,^{61,62} Ladanyi and Stratt conclude that the symmetry differential of the solute–solvent ground and excited state interactions determines the relative effectiveness of translational versus rotational solvent motions during initial solvent relaxation. This scaling argument predicts that translational solvent motions play the greatest role for the case of a spherically symmetric differential interaction while rotational motions are more important for dipolar symmetry. Thus, a major role for translation is consistent with the mechanical expansion of the hydrated electron at short times associated with the differential between the ground and excited states, while the increased evidence for libration in the individual state energies (cf. Fig. 2) is consistent with charge distribution fluctuations of leading dipolar symmetry.

Figure 3 explores the isotope effect on the nonequilibrium solvation dynamics of the hydrated electron. In computing solvent response functions from Eq. (2), we note that while $U(0)$ is well determined by the resonance condition for excitation, there is an ambiguity concerning the choice of $U(\infty)$. For classical normal and deuterated water, we expect the equilibrium excited state energy gaps to be identical. In D₂O, however, the simulated excited state lifetime is roughly twice as long as that in H₂O, as discussed in more detail in Sec. IV. Thus, the solvent response on time scales longer than the excited state lifetime in H₂O causes continued re-

TABLE I. Parameters for nonlinear least-squares fits (dashed curves) of a Gaussian plus biexponential decay: $a \exp[-1/2(t/\tau_g)^2] + b \exp[-t/\tau_1] + c \exp[-t/\tau_2]$ to solvent response functions shown (solid and dotted curves) in Fig. 3. Times are given in fs; numbers in parenthesis show the amplitude of the corresponding component. The long time in H₂O was determined from the decay of the calculated spectral transients; see the text.

Solvent	τ_g (fs)	τ_1 (fs)	τ_2 (fs)
H ₂ O	24 (0.38)	240 (0.62)	1100(0.0)
D ₂ O	26 (0.44)	295 (0.30)	1100(0.26)

laxation of the quantum gap in D₂O past that observed in H₂O. To calculate the equilibrium gap in D₂O, we averaged configurations from all trajectories where the electron occupied the excited state for times greater than 2 ps, and determined a 0.45 eV value for the asymptotic energy gap. This value indeed indicates further solvent relaxation than the 0.56 eV value we obtained in our previous work in H₂O, where we could not explore times significantly greater than 1 ps due to the short excited state lifetime.⁷ Were we able to correctly capture the later solvation dynamics in normal water with a longer-lived probe, it would be expected to have the effect of adding a tail and then raising the H₂O solvent response function (solid curve) in Fig. 3 until the tail just about overlaps with the tail of the D₂O solvent response (dotted curve).

Having noted this missing longest time solvent response in H₂O, Fig. 3 shows that the solvent responses in H₂O and D₂O are actually quite similar. The inset shows the short time responses of the two solvents in detail. Both are characterized by a rapid Gaussian decay⁶³ comprising roughly half of the response, followed by exponential relaxation on longer time scales. Both the Gaussian response and more notably the subsequent exponential decay in D₂O are slightly slower than those in H₂O, but the curves are similar enough that it would be very difficult to separate them experimentally with limited time resolution. The dashed curves in Fig. 3 represent Gaussian plus biexponential fits to the solvent response functions, with parameters summarized in Table I. The longest time entry in Table I for H₂O comes from exponential fits to the decay of the spectral transients; the long time solvent response still has some spectroscopic manifestation even though it has nominally 0% amplitude in the decay of the quantum energy gap. The Gaussian component shows a $\leq 10\%$ isotope effect, corresponding well with our interpretation of predominantly translational modes being displaced upon photoexcitation. The faster exponential decay shows a 23% increase upon deuteration, in excellent accord with expectations based on the experimental isotope change in water's longitudinal dielectric relaxation time of 26%. Our assignment of the experimental spectral transients from Barbara's group^{27,28} is slightly modified from our previous work: the observed 300 fs decay is predominantly a manifestation of the fast exponential solvation dynamics, whereas the 1.1 ps decay reflects a mixture of nonadiabatic relaxation and the slower exponential solvation dynamics which both occur on similar time scales. The details of this spectral assignment are discussed in Sec. V.

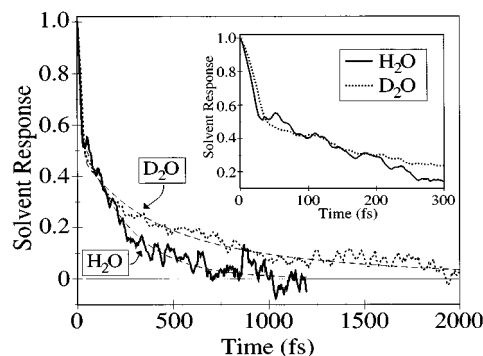


FIG. 3. The isotope effect on the nonequilibrium solvent response [Eq. (2)] following photoexcitation of the hydrated electron. The solid curve shows solvation dynamics in H₂O (Ref. 7), while the dotted curve displays the solvent response in D₂O. The dashed lines show Gaussian plus biexponential fits to the solvent response functions with parameters summarized in Table I. The inset exhibits the early time portion of the two responses on an expanded scale for better comparison of the Gaussian inertial components.

We have already compared the solvent response function for the photoexcited solvated electron in H₂O to previous work on aqueous solvation dynamics,⁷ but the solvent response in D₂O and the nature of the isotope effect merit further comparisons to other theoretical studies in the literature. Fonseca and Ladanyi investigated the isotope effect in the early time solvation response of methanol, and found a change in the Gaussian inertial decay time which was smaller than that expected for purely rotational motion of the hydroxyl hydrogen alone.⁶⁴ This finding is in accord with our results for water, where a $\sqrt{2}$ dependence of the decay time would have been expected for inertial solvent molecular motions which involved reorientation of the water dipole. Perhaps the most similar study to ours is that of Barnett, Landman, and Nitzan,¹⁴ who used a similar model of the hydrated electron to study the adiabatic relaxation following excitation in both normal and deuterated water. In contrast to our results, these workers did find a $\sim\sqrt{2}$ isotope effect on the initial Gaussian decay, and thus suggested that this early time portion of the solvation response was due to water reorientation motions. Barnett *et al.* based their conclusions, however, on the results of only two trajectories, and thus were not able to comment on the presence of an isotope effect in the longer time relaxation.¹⁴ Given the difference in statistics between our simulations and theirs, it is difficult to determine if our results are truly at odds. Our results are also in general accord with the molecular hydrodynamic theory of Nandi, Roy, and Bagchi,⁶⁵ who predict solvent response functions for water based on experimental dielectric dispersion data as input. These workers find essentially no change in the initial Gaussian relaxation upon deuteration, but do see a small isotope effect in the long time exponential tails similar to that observed in Fig. 3. The theory used in these studies assigns the initial Gaussian decay to the relaxation of long wavelength polarization modes of the solvent.⁶⁶ The quantitative agreement between our results and the theory of Nandi *et al.*, however, is not as satisfactory. The theory, which agrees well with the experimental aqueous solvation

measurements of Jimenez *et al.*,⁶⁷ predicts a Gaussian decay which is twice as long as that observed here, and exponential decay time scales which are significantly faster than ours. As discussed below, these differences may be due to the role of mechanical forces in the solvation dynamics in the present case, and which are not accounted for in this theory.

There have also been several experimental studies on the isotope effect in solvation dynamics. Barbara *et al.* have measured the solvation dynamics of a coumarin probe in both light and heavy water.⁶⁸ Although these workers were unable to resolve the inertial dynamics, they did observe a ~30% isotope effect on the exponential portions of the solvent response, results which match well with our Fig. 3. In addition to their high time resolution study in H₂O,⁶⁷ Jimenez and Fleming have also explored solvation dynamics in D₂O.⁶⁹ Although to the best of our knowledge they have not fully analyzed their D₂O data, the individual fluorescence traces suggest little change in the inertial or longer exponential time scales, but a slight increase in the shorter exponential time scale in accord with our results. Miller's group⁵² and Castner *et al.*⁵¹ have measured the optical Kerr effect in water, and Miller's group has limited data in deuterated water as well. Like the results of Jimenez and Fleming, Miller reports the only significant change upon deuteration taking place in the intermediate time scales of the response.⁷⁰ Finally, Pal *et al.* have recently explored the solvent responses of aniline and *N,N*-dimethylaniline (DMA) and their deuterated analogs.⁷¹ Neither solvent shows any inertial dynamics, so the results are only on the diffusive, exponential relaxation components. Fully deuterated aniline displays the same isotope effect as aniline deuterated solely on the amino group, suggestive of specific hydrogen bonding interactions in the solvation process. Surprisingly, DMA shows no isotope effect at all. Overall, all the available experimental evidence suggests that the details of the solute-solvent coupling are important in determination of the isotope effect in solvation dynamics.

IV. THE COUPLING BETWEEN SOLVATION AND NONADIABATIC RELAXATION

Because the solvent-induced fluctuations of the quantum energy levels of the photoexcited hydrated electron are comparable to the spacing between them, a nonadiabatic description of the electronic dynamics is essential. The 20 nonadiabatic trajectories run in D₂O show a wide dispersion of nonadiabatic transition times; by considering the entire swarm of trajectories, valuable insight can be gained into the nature of the interplay between solvation dynamics and nonadiabatic relaxation. The solid curves in Fig. 4 display the probability for remaining in the excited state for the entire set of D₂O trajectories as well as the survival probability for our earlier results H₂O.⁷ Because 20 trajectories were run for each of the two solvents, the survival curves jump in steps of 0.05 each time a single trajectory undergoes radiationless relaxation. Table II summarizes the median and average values of the survival time for each of the two systems.

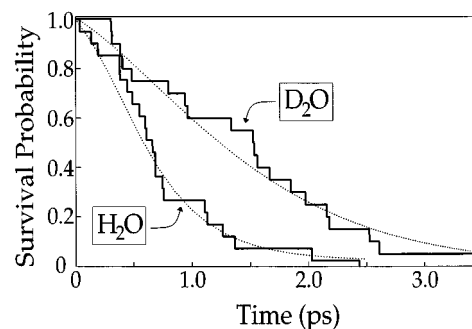


FIG. 4. The isotope effect on the excited state survival probability as a function of time. The solid curves denote the fraction of trajectories in which the electron still resides in the excited state. The dashed curves are fits to a simple one-parameter model which assumes an inverse linear coupling between the quantum energy gap, controlled by solvation, and the nonadiabatic relaxation rate. See the text, Eq. (3), and Table II.

As is also obvious from inspection of Fig. 4, the average survival time in D₂O is roughly twice that in H₂O.

The average and median survival times presented in Table II reflect a mixture of different inherent nonadiabatic transition rates and differing solvation dynamics between the two solvents. In our earlier work,⁷ we presented a simple model for the decay of the survival probability which assumed an inverse linear dependence on the quantum energy gap

$$\frac{dP(t)}{dt} = -P(t)/\tau U(t), \quad P(0)=1 \quad (3)$$

where $P(t)$ is the fraction of population in the excited state at time t after excitation, $U(t)$ is the time-dependent quantum energy gap normalized to the size of the equilibrium excited state gap after completion of the solvation response, and the proportionality constant τ is simply the equilibrium excited state lifetime. Equation (3) is in general accord with our physical intuition: immediately after photoexcitation when the gap is large, the nonadiabatic transition rate is small. The nonradiative transition rate then increases with time as the gap decreases due to solvation, and does not reach its maximum, equilibrium value until after the solvation response is complete.⁷² At long times, τ is simply the time scale for exponential decay. This variation in the rate with solvation forms the basis for the differences between earlier experiments and simulations studying the relaxation of electrons photoinjected into neat water¹⁹⁻²⁶ and the photoexcitation of equilibrium electrons considered here.⁷ Using

TABLE II. Characteristic nonadiabatic decay times (Fig. 4) for the photoexcited solvated electron in H₂O and D₂O. The equilibrium excited state lifetimes are determined by nonlinear least-squares fits (dotted curves, Fig. 4) to Eq. (3) using the solvation dynamics shown in Fig. 3.

Solvent	Median time (fs)	Average time (fs)	Equilibrium lifetime τ Eq. (3)
H ₂ O	630	730	450
D ₂ O	1530	1470	850

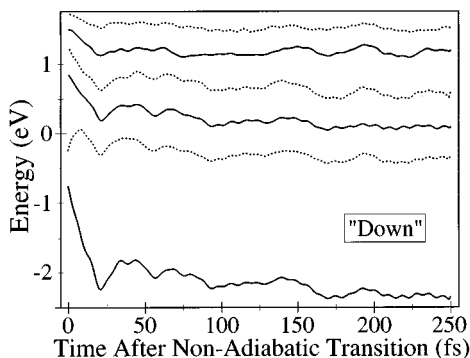


FIG. 5. Ensemble averaged adiabatic eigenstates (alternating solid and dashed curves) for configurations immediately following the nonadiabatic transition in each nonequilibrium trajectory. The initial configuration (time zero) starts at a different point following photoexcitation for each trajectory; the distribution of starting times is given by the survival curve in Fig. 4.

the fits to the time-dependent quantum energy gaps summarized in Table I, Eq. (3) can be solved numerically for $P(t)$, leaving the equilibrium survival rate τ as the only adjustable parameter. Nonlinear least-squares fits to the survival curves, shown as the dotted lines in Fig. 4, give a best fit value for the equilibrium transition rate in D₂O which is about twice that in H₂O (see Table II). The simple model represented by Eq. (3) does a good job of capturing the decay dynamics in both solvents.

The large difference in the nonradiative decay rates between light and heavy water is a direct reflection of the role of nuclear velocities in the nonadiabatic coupling. The fastest nuclear velocities in D₂O are $\sqrt{2}$ times smaller than in H₂O, and thus for identical quantum coherence times the coupling between the states is roughly twice as small in D₂O versus H₂O.³³ As mentioned in Sec. I, however, the experimental results show essentially no isotope dependence to the transient spectroscopy following photoexcitation, suggesting that both the nonadiabatic transition rates and the solvation dynamics are similar for the electron in H₂O and D₂O.^{27–29} We recently have rationalized the difference between the experimental and simulation results by considering the role of quantum decoherence in the two solvents.³³ We found that the quantum coherence time for the solvated electron in D₂O was roughly 50% longer than in H₂O. Thus, the smaller nonadiabatic coupling in D₂O adds coherently for a longer time than in H₂O, with the net result being essentially identical nonadiabatic transition rates in the two solvents. In Sec. V, we will calculate spectroscopic transients for the electron in D₂O enforcing an identical equilibrium nonadiabatic lifetime to that in H₂O. We find that if the nonadiabatic transition rates are similar, the differences in solvation dynamics are not readily detectable spectroscopically at 300 fs time resolution (cf. Fig. 3), providing an explanation for the complete lack of isotope effect observed experimentally.

To gain further insight into the response of the solvent following nonadiabatic relaxation, we show the change in the quantum energy levels of the hydrated electron following the nonadiabatic transition in Fig. 5. In constructing this figure,

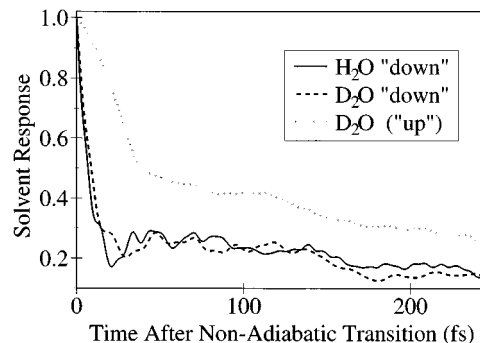


FIG. 6. The isotope effect on the nonequilibrium solvent response functions following nonadiabatic relaxation of the hydrated electron. The solid and dashed curves show the reestablishment of the ground state equilibrium for the electron in light and heavy water, respectively. The light dotted curve depicts the nonequilibrium response following photoexcitation in deuterated water (same as in Fig. 3) for comparison.

we have defined the zero of time to be the point at which the nonadiabatic transition occurs in each individual trajectory. This is a fairly unusual kind of ensemble average: while many of the initial configurations start after radiationless transition from the equilibrated excited state, some initial configurations result from excited state trajectories in which the solvation response is not yet complete. After radiationless decay over an average gap size (at the point of the nonadiabatic transition) of ~ 0.65 eV, solvent relaxation rapidly lowers the energy of the newly occupied ground state, with most of the response completed within 25 fs. There is evidence for slower relaxation of the ground state on longer time scales, but this slower component of the response plays a much smaller role. Within a few hundred fs of the nonadiabatic transition, the equilibrium structure of the hydrated electron is completely established. This rapid evolution to equilibrium once the ground state becomes occupied is in agreement with the results of previous adiabatic⁶ and nonadiabatic^{19,20} calculations, and is in accord with our general assignment of the transient spectroscopy in water to solvation dynamics followed by nonadiabatic relaxation rather than vice-versa.^{7–9}

One interesting feature of the downwards ensemble average lies in the smoothness of the traces present in Fig. 5. The energy levels of the individual trajectories (cf. Fig. 1) fluctuate by ~ 0.5 eV on a rapid time scale due to coupling with various modes of the solvent. The lack of large amplitude oscillations on the average indicate that there are no simple special motions of the solvent which can be singled out as responsible for driving the nonadiabatic dynamics.¹³ The fact that many modes of the solvent are simultaneously involved in coupling the energy levels of the hydrated electron nonadiabatically is discussed in detail elsewhere.⁷³

Figure 6 presents a comparison of the nonequilibrium solvent response functions [Eq. (2)] for both the photoexcitation (“up”) and nonadiabatic (“down”) transitions. The two traces are markedly different: the inertial component for the downwards transition is significantly faster and accounts for a much larger percentage of the total solvation response

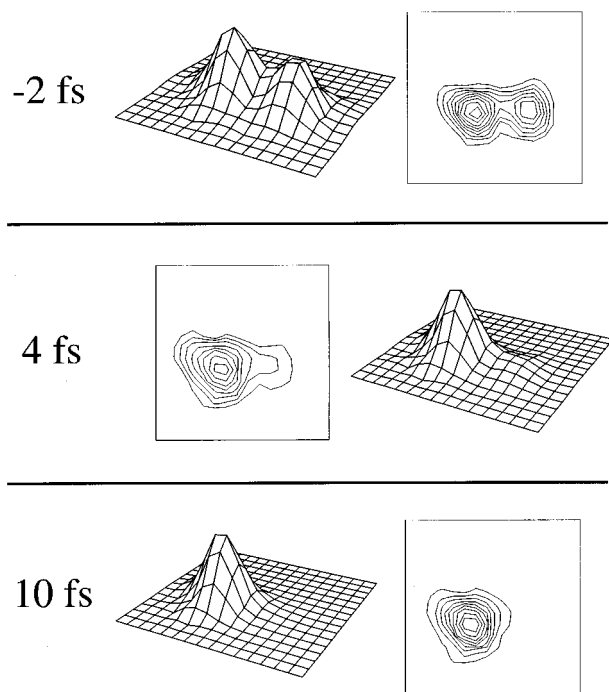


FIG. 7. Selected ground state eigenfunctions from a single trajectory, shown in perspective and as contour plots, demonstrating dynamic evolution of the solvent cavity around the electron in deuterated water following nonadiabatic relaxation. The plane of these two-dimensional slices contains both the electron center of mass and the transition dipole vector connecting the ground and first excited states. The times are relative to the nonadiabatic transition; thus, the upper plot at -2 fs displays the unoccupied ground state while the lower two plots at positive times show the now newly occupied ground state.

than that following photoexcitation. This difference bears a striking resemblance to that observed by Maroncelli and Fleming in their studies of atomic solutes in water:⁵⁶ their nonequilibrium solvent response upon ionization of the neutral solute is very similar to our “upwards” response, while their solvent response following neutralization of the ionic solute closely matches our “downwards” transition, as discussed further below. Moreover, when one computes the linear response prediction for the equilibrated excited state (by calculating the autocorrelation of the quantum energy gap [Eq. (1)] for a single long trajectory on the equilibrated excited state with the surface hopping algorithm shut off), one finds that the nonequilibrium downwards response presented in Fig. 6 is in excellent agreement with the linear response prediction. Thus, even though the two responses are clearly different due to the different nature of the microscopic solvent configuration around the electron in different electronic states, both the upwards and downwards transitions follow linear response.⁷⁴ This phenomenon will be explored further in an upcoming publication.⁷⁵

In Fig. 7, we examine how diverse initial microscopic solvent configurations can lead to very different solvent responses by using the wave function of the solvated electron as a probe of the local solvent structure. The times indicated in Fig. 7 are relative to the nonadiabatic transition point in a single trajectory. As in our previous work,⁷ the wave func-

tion depicted is the ground state eigenfunction of the electron, which is unoccupied before the radiationless transition (upper frame) but becomes the occupied state following nonadiabatic decay (lower two frames). The two-dimensional slices of the wave function shown here contain both the electron center of mass and the transition dipole vector connecting the ground and first excited states, which points along the approximately cylindrical symmetry axis of the excited state electron. The absolute orientation and position in the lab frame is the same for all three slices. Figure 7 shows both changes in the electronic charge density due to solvent motions and provides an explicit measure of the shape of the solvent cavity in which the electron resides.

Preceding the nonadiabatic transition, we observe oscillations of electron density between the lobes of the elongated peanut-shaped wave function, and the nonadiabatic transition probability to the ground state increases when the wave function becomes more asymmetric.⁷³ The occupied excited state wave function has opposite signs in each of the lobes, whereas the nodeless ground state wave function has only a single sign. It is those solvent motions which drive electron density toward only one of the two lobes that breaks this symmetry, leading to a finite probability for making a nonadiabatic transition.⁷³ The upper frame in Fig. 7 captures such a charge density asymmetry 2 fs before the nonadiabatic transition takes place; the left-hand lobe of the wave function contains significantly more charge density than the right-hand lobe. We note that similar oscillations have been observed by Space and Coker in their study of solvated electrons in liquid helium.⁷⁶

Following the nonadiabatic transition, the solvent quickly reorganizes to produce the equilibrium ground state hydrated electron, which has an *s*-like wave function about the size of one of the lobes of the equilibrium excited state electron. Of special significance, the transition initially produces an asymmetric ground state wave function which has most of its charge density in one of the original two excited state lobes. This leaves a void in the solvent which was formerly occupied by the other lobe of the excited state electron. Solvent molecules rush in to fill this void, pushing out what little electron density remains. The center panel in Fig. 7 shows that only 4 fs after the internal conversion, the electron almost entirely occupies the left-hand lobe. After only 10 fs, solvent has relaxed to produce an electronic species which has most of the characteristics of the equilibrium ground state except perhaps for a slight increase in overall size. The fact that entire solvent molecules move to fill in the void during this time is also supported by the very small isotope effect seen in Fig. 6; the initial downward solvent response does not show the $\sqrt{2}$ isotope dependence that would be characteristic of water rotational motions. Thus, we see that translational modes of the solvent are also important in relaxing the ground state charge distribution following nonadiabatic relaxation, although different time scales are critical.

This idea of predominantly displacing different translational modes upon photoexcitation and nonadiabatic relaxation leads to an appealing microscopic picture for the cou-

pling of the mechanical and dielectric solvent responses. Viscoelastic solvent relaxation occurs for solutes that undergo a change in size or shape upon excitation, even if such excitation is not accompanied by a change in charge distribution.⁷⁷ In cases where changes in both size and shape and charge distribution occur, such as the hydrated electron, the viscoelastic and dielectric solvent responses can couple together.¹³ Upon photoexcitation, the hydrated electron continuously expands along the long cavity axis pushing solvent molecules away from the ends of the lobes, and solvent molecules also translate into the void created in the nodal region. Of course, solvent reorientational motions do aid in accommodating the new excited state charge distribution, but the initial solvent motions displaced are predominantly translational, as evidenced by the small isotope effect on the inertial response (Fig. 3) and the pronounced ringing observed at translational frequencies in the calculated ultrafast spectroscopy (cf. Fig. 11 and Refs. 8–10). Following nonadiabatic relaxation, the solvent molecules are already properly orientationally aligned around the lobe that will be occupied after the transition, so only free translational motion of water molecules into the newly created void is necessary to produce significant relaxation. This causes the large difference in solvation rates for the two types of transitions (Fig. 6); following photoexcitation, first shell solvent molecules are being mechanically forced into other solvent molecules, which hinders their translational and rotational degrees of freedom. Following nonadiabatic relaxation, solvent molecules near the unoccupied lobe simply move into the void, where they can easily take up configurations that lower the energy of the ground state.

In both the photoexcitation and nonadiabatic cases, a major portion of the relaxation is due to the mechanical forces between the solute and the solvent. Recent hole-burning studies finding nearly identical solvation dynamics for both polar and nonpolar solutes in propylene carbonate point to the importance of mechanical forces in solvation.⁷⁸ Simulation work has also indicated the importance of mechanical interactions in solvent relaxation.^{79,80} A similar phenomenon has also been noted by Maroncelli and Fleming in their atomic solute simulations.⁵⁶ Following ionization of a neutral solute, solvent dipoles aligned for the neutral species can reorient to favorably solvate the new charge distribution. Following neutralization of a charged solute, solvent molecules which were pulled in towards the solute by the Coulomb attraction now find themselves on a highly repulsive part of the potential due to (mechanical) Pauli exclusion forces. The solvent molecules are rapidly pushed away; small solvent motions cause the solvation energy to drop considerably due to the steepness of the repulsive part of the potential. The situation is nearly identical for the hydrated electron. The small recurrence after the initial relaxation in the downwards solvent response (Fig. 6) provides some evidence for reorientational motion subsequent to the initial translation. This oscillation occurs at the period of the librational frequency, and shows the $\sqrt{2}$ isotope dependence expected for reorientational motion in water.

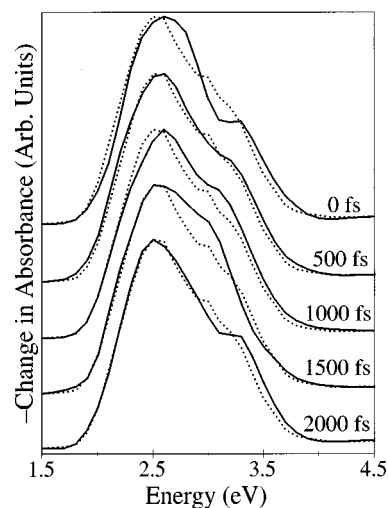


FIG. 8. Transient bleach dynamics for the solvated electron in deuterated water at various time delays after photoexcitation (solid curves), normalized to equal area with the equilibrium ground state absorption spectrum (dashed curves) for reference.

V. ULTRAFAST TRANSIENT SPECTROSCOPY OF THE SOLVATED ELECTRON IN D₂O

One of the principle advantages of utilizing a quantum model for the hydrated electron is the opportunity to make a direct connection with experiment by using the wave functions to calculate spectroscopic observables. In previous work,^{8–10} we found excellent agreement between spectroscopic transients calculated with this model of the hydrated electron and the experimental results of Barbara and co-workers.^{27–30} By dissecting the calculated transients into individual bleach, absorption, and emission components, we were able to elucidate how the solvent motions responsible for solvation dynamics and nonadiabatic relaxation are reflected spectroscopically.^{8,9} In this section, we examine the experimental manifestations of the isotope effect by studying these same spectral components for the solvated electron in deuterated water and comparing to our previous results in normal water.

The solvent motions which couple to the energy levels of the hydrated electron fluctuate on a variety of time scales. The laser pulse used for photoexcitation is faster than some of these fluctuations. Thus, only that fraction of the population which are in instantaneous configurations such that their quantum energy gap is resonant with the laser pulse are photoexcited. This leaves an absorption deficit centered around the frequency of the excitation laser, which eventually broadens into the entire equilibrium absorption spectrum as the longer time fluctuations cause this select population to sample all possible configurations, the so-called spectral diffusion. The dynamics of this ground state bleach, or transient hole, play an important role in the total ultrafast pump–probe spectroscopy of the hydrated electron.^{8,9,81}

Figure 8 shows the calculated transient bleach spectra³⁶ for the solvated electron in D₂O following photoexcitation at ~ 2.3 eV at various time delays (solid curves). The calculated equilibrium absorption spectrum, which would have been

produced by uniform bleaching of the entire band, is shown normalized to equal area at each time delay (dotted curves) to emphasize the shape of the hole. Within the statistical noise, the transient bleaching spectroscopy for the solvated electron in deuterated water is identical to that observed previously in normal water.^{8,81} Rapid solvent fluctuations cause the initial hole ($t=0$) to be quite broad, although there is some extra bleaching on the red edge of the spectrum near the frequency of the excitation laser. The red edge of the spectrum undergoes a slight blueshift at longer time delays, and the bleach becomes indistinguishable from the equilibrium absorption spectrum by delays of 2 ps.

At first glance it seems surprising that the bleaching dynamics are not affected by isotopic substitution. The fast solvent fluctuations, however, are faster than the inverse of the absorption linewidth (fast modulation limit)⁸² in both H₂O and D₂O, so there is no isotope effect on the shape of the initial hole. In previous work studying the polarized hole-burning spectroscopy of the hydrated electron,¹⁰ we found that in addition to the fast isotropic fluctuations, slower anisotropic solvent fluctuations couple to the electron which relax on the picosecond time scale. This is a consequence of the fact that it takes several picoseconds to randomize the orientation of the long axis of the cavity enough so that the 3 p -like excited states interchange roles. The blueshifting spectral dynamics along the red edge of the spectrum reflect this slow reorientation. We find that both the transition dipole orientational autocorrelation function and the polarized transient bleaching spectroscopy are identical for the solvated electron in both H₂O and D₂O. Thus, the long time fluctuations which randomize the cavity orientation involve solvent motions which are not significantly affected by isotopic substitution. We expect that rather than a rotation of the electron and its first solvent shell, electronic reorientation takes place due to a pseudorotation associated with structural rearrangement of the solvent cavity.^{10,30} This structural rearrangement would involve the diffusive motion of many solvent molecules. In this case, a measurable isotope effect on the ground state bleach would not be expected.

In addition to the bleaching of the ground state, those electrons promoted to the excited state can absorb light either before or after they undergo radiationless relaxation. The calculated transient absorption component for the photoexcited solvated electron in D₂O is presented in Fig. 9(a). The early time increase in absorption intensity is the result of convolution with the 300 fs instrument response function. The zero time spectrum reflects the nascent absorption of the excited state, and the subsequent dynamics reflect a mixture of spectral evolution of the excited state absorption due to solvation dynamics and the reestablishment of the equilibrium spectrum following the nonadiabatic transition. The thin solid line shows the equilibrium absorption of the ground state for comparison. Like the absorption spectra previously calculated for the electron in H₂O,⁸ the red peak of the excited state absorption spectrum in D₂O undergoes a redshift as the oscillator strength to the other two p -like excited states increases with solvation, and the spectrum shows a dynamic blueshift in the high energy spectral tail.

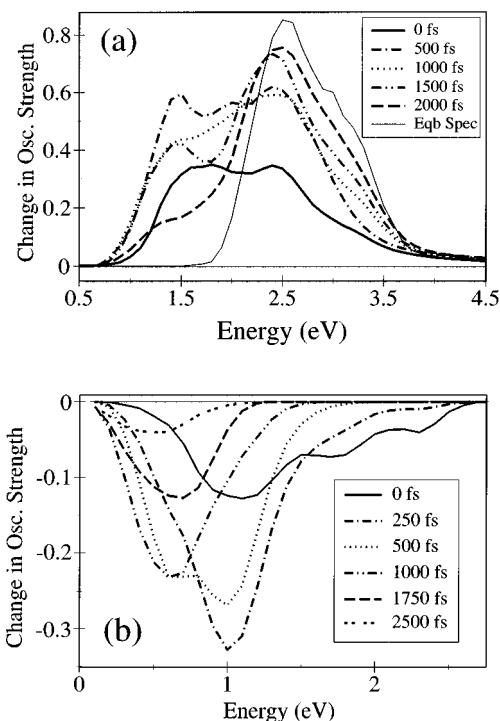


FIG. 9. (a) Transient absorption spectral component for the solvated electron in deuterated water at various time delays after photoexcitation in absolute intensity units. These spectra include contributions from both excited state electrons and electrons that have nonadiabatically returned to the ground state. The thin solid line shows the equilibrium ground state absorption for reference. (b) Stimulated emission spectral component for the solvated electron in deuterated water at various time delays following photoexcitation in absolute intensity units.

The final component to the complete transient spectroscopy of the photoexcited solvated electron in D₂O, due to stimulated emission, is shown in Fig. 9(b). Like the emission component in H₂O,⁸ the initial spectrum is broad and redshifted from the excitation wavelength due to convolution of the instrument function with the inertial portion of the solvent response. The emission then narrows with time and undergoes a dynamic Stokes shift due to solvation, processes which have been analyzed in detail for the case of H₂O in previous work.^{8,11} The only differences between the emission dynamics in H₂O and D₂O result from the longer simulated excited state lifetime which brings to light the presence of the slower solvation component in the deuterated solvent. The lifetime difference is manifest in greater emission intensity at longer times in D₂O than in H₂O. The presence of the slow solvation component is evident in the continued Stokes shift of the emission in D₂O at very long times: the long time emission spectrum in D₂O (2.5 ps) has its maximum near 0.5 eV, roughly 0.2 eV further redshifted from the corresponding maximum at long times (1.5 ps) in H₂O. Other than these few differences, the emission dynamics are essentially the same for the excited state electron in light and heavy water, reflecting the generally similar solvent response functions (Fig. 3) of the two solvents.

Figure 10 shows the complete transient spectroscopy of the solvated electron in deuterated water following photoex-

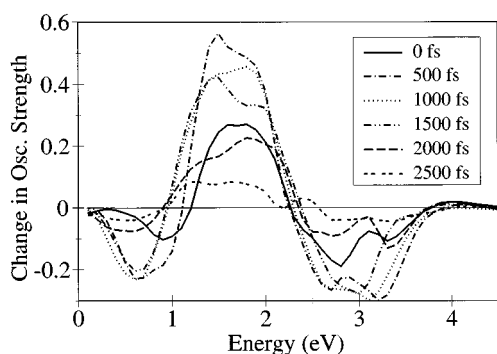


FIG. 10. Complete change in absorption for the solvated electron in deuterated water at various time delays after photoexcitation in absolute intensity units. These spectra are the sum of those shown in Figs. 8, 9(a), and 9(b).

citation at 2.3 eV. These spectra are the sum of the individual ground state bleach, transient absorption and stimulated emission components presented in Figs. 8 and 9. Like the spectroscopy in H₂O,^{8,9} the bleaching component dominates the total spectroscopy to the blue of 2.5 eV, the excited state absorption is evident in the 1.5–2.0 eV region, and stimulated emission plays the important role to the red of 1.0 eV. The complete transient spectroscopy shows a dynamic blueshift in the 2.0–2.5 eV region, due to superposition of the blueshifts of both the red edge of the bleach and the blue shoulder of the transient absorption. The total spectral dynamics also show a redshift in the 0.8–1.3 eV region, due to the redshifting excited state absorption and the dynamic Stokes shift of the stimulated emission. The principal difference in the total spectroscopy between H₂O and D₂O lies in the recovery time scale; the slower excited state relaxation in D₂O leads to spectral transients which are more persistent than those in H₂O by nearly a factor of 2.

Although the results presented in Fig. 10 compare quite favorably with experiment,⁸³ the simulated isotope effect on the transient spectroscopy is not in good agreement with the experimentally measured femtosecond results. The experiments show identical spectral features in H₂O and D₂O,^{28,29} in sharp contrast to the nearly factor of 2 difference in recovery time predicted by the present simulations. This difference is predominantly due to the difference in calculated lifetimes resulting from incorrectly estimating the decay of quantum decoherence in the algorithm used for nonadiabatic dynamics. Since a correct treatment of quantum decoherence should produce essentially identical nonadiabatic relaxation rates,³³ a better comparison between the simulations and experiment can be made by correcting the lifetime in D₂O to match that in H₂O. By reweighting the calculated spectral transients from each trajectory to reflect the corrected lifetime, we can determine whether or not the simulations predict if differences in solvation dynamics between H₂O and D₂O are observable spectroscopically. Corrected population dynamics for the electron in heavy water can be determined by Eq. (3) using the known behavior of the quantum energy gap $U(t)$ of the electron in D₂O (Fig. 3) but the equilibrium excited state lifetime τ determined in H₂O (450 fs). The re-

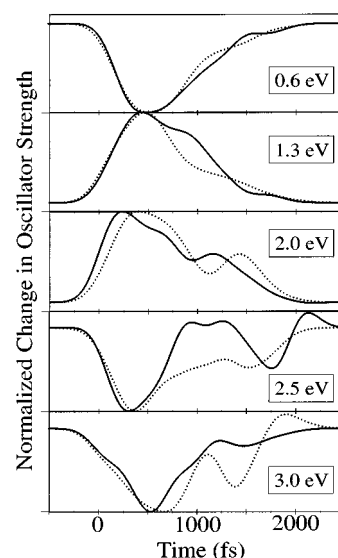


FIG. 11. Time domain spectral transients for the solvated electron in deuterated water (dotted curves) corrected for the case that the equilibrium nonadiabatic transition rate is the same as that in normal water (see the text). The solid curves show spectral transients for the same wavelengths in normal water (Ref. 8) for comparison. All the transients shown have been normalized to the same maximum amplitude.

sulting survival curve is quite similar to that observed in H₂O, although slightly longer lived due to the differences in solvation dynamics between the two solvents. The excited state contributions to the total spectroscopy for the D₂O trajectories are then reweighted by the corrected survival probabilities, and the three spectral components readded together. This produces calculated spectral dynamics for the electron in D₂O with the correct underlying solvation dynamics and the corrected excited state lifetime, which matches that in H₂O. These corrected D₂O transients (dashed curves) are compared to those calculated previously for H₂O (solid curves) in Fig. 11.

As is evident from Fig. 11, the H₂O and corrected D₂O calculated spectral transients are remarkably similar within the noise of the simulations. As discussed elsewhere, the low frequency oscillations superimposed on the transients reflect the low frequency solvent translational motions which are displaced upon photoexcitation and are likely not statistically significant.^{8,9} The D₂O transients appear to rise a little more slowly than the H₂O transients, due to the slower longitudinal component of the solvation dynamics (Table I). At 300 fs time resolution, however, it is clear that it is quite difficult to distinguish the spectral dynamics in the two solvents. Thus, for excited state lifetimes which are equal in the two solvents, the simulations predict identical spectral transients at the presently available statistical (theoretical) and experimental time resolution. Based on the results of the simulations, however, the differences in solvation dynamics between light and heavy water should be enough to produce measurable spectroscopic changes in experiments with significantly better time resolution.

VI. CONCLUSIONS

In summary, we have investigated the solvent dynamics following photoexcitation of the solvated electron in D₂O, and compared the results to similar work in H₂O. The nonadiabatic relaxation and solvation dynamics are coupled together in an intimate way. The solvent spectral density couples differently to the individual electronic energy levels and the quantum energy gap, producing relaxation dynamics which cannot be predicted from the fluctuations of the individual energy levels alone. The change in symmetry of the charge distribution upon excitation is important in determining the effectiveness of the various modes in the overall solvent relaxation. A striking example of this is the large difference between the solvent responses following photoexcitation and nonadiabatic relaxation of the solvated electron. Detailed analysis of the solvent motions accompanying radiationless relaxation point out the importance of short-range mechanical forces as well as the longer range Coulomb forces in the overall solvent response.

The overall solvent responses following photoexcitation in H₂O and D₂O are remarkably similar (Table I), but the longer simulated excited state lifetime in D₂O allows direct observation of a slower relaxation component. The excited state lifetime in heavy water is found to be roughly a factor of 2 larger than in normal water. Part of this isotope effect on the transition rate is due to the slower solvation dynamics in D₂O which keeps the energy gap large for a longer time than in H₂O. The majority of this isotope effect on the lifetime, however, reflects the smaller nonadiabatic coupling in D₂O. The solvent response following nonadiabatic relaxation in the two solvents are essentially identical, reflecting the importance of mechanical forces and reinforcing the concept of the rapid establishment of equilibrium following return to the ground state.

Experiments at 300 fs time resolution find no significant differences in spectral evolution following photoexcitation of the solvated electron in H₂O and D₂O. This indicates that both the solvation and nonadiabatic relaxation dynamics are similar in the two solvents. A detailed theoretical analysis suggests that the simulated excited state lifetime should be comparable in light and heavy water if the quantum decoherence times were chosen correctly.³³ Calculations correcting the equilibrium lifetime in D₂O to match that in H₂O reproduce the nearly identical spectral transients in the two solvents, indicating that the simulations have captured the essential physics following photoexcitation of the hydrated electron. The simulations further indicate that experiments with sufficient time resolution (≤ 50 fs) should be able to resolve small isotopic differences in the solvation dynamics and/or excited state lifetimes in the two solvents.

ACKNOWLEDGMENTS

This work was supported by the National Science Foundation. B.J.S. gratefully acknowledges the support of a NSF Postdoctoral Fellowship in Chemistry, and the allocation of computational resources from the San Diego Supercomput-

ing Center. We thank Paul Barbara, Peter Walhout, and Carlos Silva for freely sharing their data and ideas on the issues discussed here.

- ¹M. Maroncelli, *J. Mol. Liq.* **57**, 1 (1993).
- ²P. J. Rossky and J. D. Simon, *Nature* **370**, 263 (1994).
- ³P. F. Barbara and W. Jarzeba, *Adv. Photochem.* **15**, 1 (1990).
- ⁴D. F. Coker, in *Computer Simulations in Chemical Physics*, edited by M. P. Allen and D. J. Tildesely (Kluwer Academic, Dordrecht, 1993), p. 315.
- ⁵J. Schnitker, K. Motakabbir, P. J. Rossky, and R. A. Friesner, *Phys. Rev. Lett.* **60**, 456 (1988).
- ⁶P. J. Rossky and J. Schnitker, *J. Phys. Chem.* **86**, 3471 (1987).
- ⁷B. J. Schwartz and P. J. Rossky, *J. Chem. Phys.* **101**, 6902 (1994).
- ⁸B. J. Schwartz and P. J. Rossky, *J. Chem. Phys.* **101**, 6917 (1994).
- ⁹B. J. Schwartz and P. J. Rossky, *J. Phys. Chem.* **98**, 4489 (1994).
- ¹⁰B. J. Schwartz and P. J. Rossky, *Phys. Rev. Lett.* **72**, 3282 (1994).
- ¹¹B. J. Schwartz and P. J. Rossky, *J. Phys. Chem.* **99**, 2953 (1995).
- ¹²S. J. Rosenthal, B. J. Schwartz, and P. J. Rossky, *Chem. Phys. Lett.* **229**, 443 (1994).
- ¹³B. J. Schwartz and P. J. Rossky, *J. Mol. Liq.* **65/66**, 23 (1995).
- ¹⁴R. B. Barnett, U. Landman, and A. Nitzan, *J. Chem. Phys.* **90**, 4413 (1989).
- ¹⁵E. Neria, A. Nitzan, R. N. Barnett, and U. Landman, *Phys. Rev. Lett.* **67**, 1011 (1991).
- ¹⁶E. Neria and A. Nitzan, *J. Chem. Phys.* **99**, 1109 (1993).
- ¹⁷A. Staib and D. Borgis, *Chem. Phys. Lett.* **230**, 405 (1994).
- ¹⁸A. Staib and D. Borgis, *J. Phys. Chem.* **103**, 2642 (1995).
- ¹⁹F. A. Webster, J. Schnitker, M. S. Friedrichs, R. A. Friesner, and P. J. Rossky, *Phys. Rev. Lett.* **33**, 3172 (1991).
- ²⁰T. H. Murphrey and P. J. Rossky, *J. Chem. Phys.* **99**, 515 (1993).
- ²¹E. Keszei, S. Nagy, T. H. Murphrey, and P. J. Rossky, *J. Chem. Phys.* **99**, 2004 (1993).
- ²²E. Keszei, T. H. Murphrey, and P. J. Rossky, *J. Phys. Chem.* **99**, 22 (1995).
- ²³F. Long, H. Lu, and K. B. Eisenthal, *Phys. Rev. Lett.* **64**, 1469 (1990).
- ²⁴F. Long, H. Lu, X. Shi, and K. B. Eisenthal, *Chem. Phys. Lett.* **185**, 47 (1991).
- ²⁵A. Migus, Y. Gauduel, J.-L. Martin, and A. Antonetti, *Phys. Rev. Lett.* **58**, 1559 (1987).
- ²⁶Y. Gauduel, S. Pommeret, A. Migus, and A. Antonetti, *J. Phys. Chem.* **95**, 533 (1991).
- ²⁷J. C. Alfano, P. K. Walhout, Y. Kimura, and P. F. Barbara, *J. Chem. Phys.* **98**, 5996 (1993).
- ²⁸Y. Kimura, J. C. Alfano, P. K. Walhout, and P. F. Barbara, *J. Phys. Chem.* **98**, 3450 (1994).
- ²⁹P. K. Walhout and P. F. Barbara (private communication).
- ³⁰P. J. Reid, C. Silva, P. K. Walhout, and P. F. Barbara, *Chem. Phys. Lett.* **228**, 658 (1994).
- ³¹F. A. Webster, P. J. Rossky, and R. A. Friesner, *Comput. Phys. Commun.* **63**, 494 (1991).
- ³²F. Webster, E. T. Wang, P. J. Rossky, and R. A. Friesner, *J. Chem. Phys.* **100**, 4835 (1994).
- ³³B. J. Schwartz, E. R. Bittner, O. V. Prezhdo, and P. J. Rossky, *J. Chem. Phys.* **104**, 5942 (1996).
- ³⁴J. Schnitker and P. J. Rossky, *J. Chem. Phys.* **86**, 3462 (1987).
- ³⁵M. P. Allen and D. J. Tildesely, *Computer Simulations of Liquids* (Oxford University Press, New York, 1987).
- ³⁶Note that the calculated equilibrium absorption spectrum is blueshifted by ≥ 0.5 eV from the experimental one, a result likely due to the lack of inclusion of electronic polarizability of the solvent (see, e.g., Ref. 18). In previous work, we subtracted this shift in the equilibrium spectrum when comparing the experimental and calculated nonequilibrium spectral transients. In the present work, all spectral calculations are presented without this shift taken into account, directly as computed during the simulations.
- ³⁷Based on our experience in H₂O, we expected rapid equilibration following the nonadiabatic relaxation and elected to save computational resources by terminating trajectories 0.5 ps after the radiationless transition. *A posteriori* justification for this assumption is provided in Fig. 6.
- ³⁸J. C. Tully and R. K. Preston, *J. Chem. Phys.* **55**, 562 (1971).
- ³⁹P. Pechukas, *Phys. Rev.* **181**, 174 (1969).
- ⁴⁰E. R. Bittner and P. J. Rossky, *J. Chem. Phys.* **103**, 8130 (1995).
- ⁴¹K. Toukan and A. Rahman, *Phys. Rev. B* **31**, 2643 (1985).

- ⁴²R. W. Impey, P. A. Madden, and I. R. McDonald, *Mol. Phys.* **46**, 513 (1982).
- ⁴³I. M. Svishchev and P. G. Kusalik, *J. Phys. Chem.* **98**, 728 (1994).
- ⁴⁴O. Telemann, B. Jonsson, and S. Engstrom, *Mol. Phys.* **60**, 193 (1987).
- ⁴⁵Note that this isotope effect is significantly larger than would be expected on the simple basis of scaling like total mass^{1/2}. This is likely the result of significant translation-rotation coupling.
- ⁴⁶See, e.g., G. S. Delbuono, P. J. Rossky, and J. Schnitker, *J. Chem. Phys.* **95**, 3728 (1991).
- ⁴⁷F.-Y. Jou and G. R. Freeman, *J. Phys. Chem.* **83**, 2383 (1979).
- ⁴⁸M. Maroncelli and G. R. Fleming, *J. Chem. Phys.* **86**, 6221 (1987).
- ⁴⁹See., e.g., J. B. Hasted, S. K. Husain, F. A. M. Frescura, and J. R. Birch, *Chem. Phys. Lett.* **118**, 622 (1985).
- ⁵⁰G. E. Walrafen, *J. Phys. Chem.* **94**, 2237 (1990).
- ⁵¹E. W. Castner, Y. J. Chang, Y. C. Chu, and G. E. Walrafen, *J. Chem. Phys.* **102**, 653 (1995), and references therein.
- ⁵²R. D. J. Miller (private communication).
- ⁵³P. A. Madden and R. W. Impey, *Chem. Phys. Lett.* **123**, 502 (1986).
- ⁵⁴S. Sastry, H. E. Stanley, and F. Sciortino, *J. Chem. Phys.* **100**, 5361 (1994).
- ⁵⁵A calculation of the resonance Raman spectrum of the hydrated electron also bears this out: resonance enhancement is seen only for the low frequency, intermolecular solvent motions. W. B. Bosma, B. J. Schwartz and P. J. Rossky (unpublished data).
- ⁵⁶M. Maroncelli and G. R. Fleming, *J. Chem. Phys.* **89**, 5044 (1988).
- ⁵⁷It would be interesting, for example, to compare the solvation dynamics resulting from exciting a neutral-to-singly charged atomic species as explored in Ref. 56 and those resulting from excitation of a singly charged to doubly charged species. In the latter case, the orientation of the solvent is already nearly optimal for the doubly charged species, so most of the solvation should result from a slight inward collapse of the first solvation shell due to the enhanced Coulomb attraction. For this case, there would be no symmetry change to the charge distribution and hence, negligible reorientational motion in the solvent relaxation.
- ⁵⁸P. V. Kumar and M. Maroncelli, *J. Chem. Phys.* **103**, 3038 (1995).
- ⁵⁹Note that for the hydrated electron and idealized state symmetry, the leading order change in charge distribution would be the quadrupole; see Ref. 7.
- ⁶⁰B. M. Ladanyi and R. M. Stratt, *J. Phys. Chem.* **100**, 1266 (1996).
- ⁶¹R. M. Stratt and M. Cho, *J. Chem. Phys.* **100**, 6700 (1994).
- ⁶²B. M. Ladanyi and R. M. Stratt, *J. Phys. Chem.* **99**, 2502 (1995).
- ⁶³M. Maroncelli, P. V. Kumar, A. Papazyan, M. L. Horng, S. J. Rosenthal, and G. R. Fleming, in *Ultrafast Reaction Dynamics and Solvent Effects*, edited by Y. Gauduel and P. J. Rossky [AIP Conf. Proc. **298**, 310 (1994)].
- ⁶⁴T. Fonseca and B. M. Ladanyi, *J. Mol. Liq.* **60**, 1 (1994).
- ⁶⁵N. Nandi, S. Roy, and B. Bagchi, *J. Chem. Phys.* **102**, 1390 (1995).
- ⁶⁶This is not in accord with the "standard picture" of solvation, which holds that rotational motions of individual first shell solvent molecules dominate the early time solvent response.
- ⁶⁷R. Jimenez, G. R. Fleming, K. Papazyan, and M. Maroncelli, *Nature* **369**, 471 (1994).
- ⁶⁸P. F. Barbara, G. C. Walker, T. J. Kang, and W. Jarzaba, *Proc. SPIE* **1209**, 18 (1990).
- ⁶⁹R. Jimenez and G. R. Fleming (private communication).
- ⁷⁰We note that caution is warranted when extrapolating from OKE data, which reflects the solvent polarizability, to solvation dynamics, which depends on the solvent polarization. See, e.g., H. P. Deuel, P. J. Cong, and J. D. Simon, *J. Phys. Chem.* **98**, 12600 (1994).
- ⁷¹H. Pal, Y. Nagasawa, K. Tominaga, S. Kumazaki, and K. Yoshihara, *J. Chem. Phys.* **102**, 7758 (1995).
- ⁷²A different model, in which nonadiabatic relaxation happens rapidly while the gap is large and significant relaxation then takes place on the ground state is consistent with the behavior of solvated electrons in alcohols: see P. K. Walhout, J. C. Alfano, Y. Kimura, C. Silva, and P. F. Barbara, *Chem. Phys. Lett.* **232**, 135 (1995).
- ⁷³O. V. Prezhdo and P. J. Rossky, *J. Phys. Chem.* (in press).
- ⁷⁴By linear response, we mean simply that the regression of fluctuations at equilibrium is the same as the relaxation following an external perturbation. Thus, it is possible for both the upwards and downwards transitions to follow linear response, even though the two responses are dissimilar, since the final equilibrium fluctuations in the excited state can be different from the initial equilibrium fluctuations in the ground state.
- ⁷⁵A. Mosyak, L. Turi, and P. J. Rossky (unpublished).
- ⁷⁶B. Space and D. F. Coker, *J. Chem. Phys.* **96**, 652 (1992), and references therein.
- ⁷⁷M. Berg, *Chem. Phys. Lett.* **228**, 317 (1994).
- ⁷⁸J. Ma, D. Vanden Bout, and M. Berg, *J. Chem. Phys.* **103**, 9146 (1995).
- ⁷⁹J. G. Saven and J. L. Skinner, *J. Chem. Phys.* **99**, 4391 (1993).
- ⁸⁰R. Brown, *J. Chem. Phys.* **102**, 9059 (1995).
- ⁸¹K. A. Motakabbir, J. Schnitker, and P. J. Rossky, *J. Chem. Phys.* **97**, 2055 (1992).
- ⁸²R. Kubo, *Adv. Chem. Phys.* **15**, 101 (1969).
- ⁸³As noted in Refs. 7, 9, and 20, the calculated nonadiabatic lifetime for the electron in H₂O is roughly a factor of 2 too fast, likely the result of the classical model used for the water vibrations. Thus, the simulated D₂O transients which are (incorrectly) a factor of ~2 slower than the H₂O transients due to the error in choice of quantum decoherence time actually agree better with the experimental results.